arXiv:1702.07430v1 [astro-ph.SR] 24 Feb 2017

AN R-PROCESS ENHANCED STAR IN THE DWARF GALAXY TUCANA III[*]

T. T. Hansen[1], J. D. Simon[1], J. L. Marshall[2], T. S. Li[3,2], D. Carollo[4,5], D. L. DePoy[2], D. Q. Nagasawa[2],
R. A. Bernstein[1], A. Drlica-Wagner[3], F. B. Abdalla[6,7], S. Allam[3], J. Annis[3], K. Bechtol[8], A. Benoit-Lévy[9,6,10],
D. Brooks[6], E. Buckley-Geer[3], A. Carnero Rosell[11,12], M. Carrasco Kind[13,14], J. Carretero[15,16], C. E. Cunha[17],
L. N. da Costa[11,12], S. Desai[18], T. F. Eifler[19], A. Fausti Neto[11], B. Flaugher[3], J. Frieman[3,20],
J. García-Bellido[21], E. Gaztanaga[15], D. W. Gerdes[22], D. Gruen[17,23], R. A. Gruendl[13,14], J. Gschwend[11,12],
G. Gutierrez[3], D. J. James[24,25], E. Krause[17], K. Kuehn[26], N. Kuropatkin[3], O. Lahav[6], R. Miquel[27,16],
A. A. Plazas[19], A. K. Romer[28], E. Sanchez[29], B. Santiago[30,11], V. Scarpine[3], R. C. Smith[25], M. Soares-Santos[3],
F. Sobreira[11,31], E. Suchyta[32], M. E. C. Swanson[14], G. Tarle[22], A. R. Walker[25]

(DES Collaboration)
Draft version July 13, 2018

ABSTRACT

Chemically peculiar stars in dwarf galaxies provide a window for exploring the birth environment of stars with varying chemical enrichment. We present a chemical abundance analysis of the brightest star in the newly discovered ultra-faint dwarf galaxy candidate Tucana III. Because it is particularly bright for a star in an ultra-faint Milky Way satellite, we are able to measure the abundance of 28 elements, including 13 neutron-capture species. This star, DES J235532.66−593114.9 (DES J235532), shows a mild enhancement in neutron-capture elements associated with the r-process and can be classified as an r-I star. DES J235532 is the first r-I star to be discovered in an ultra-faint satellite, and Tuc III is the second extremely low-luminosity system found to contain r-process enriched material, after Reticulum II. Comparison of the abundance pattern of DES J235532 with r-I and r-II stars found in other dwarf galaxies and in the Milky Way halo suggests a common astrophysical origin for the neutron-capture elements seen in all r-process enhanced stars. We explore both internal and external scenarios for the r-process enrichment of Tuc III and show that with abundance patterns for additional stars it should be possible to distinguish between them.

[*] This paper includes data gathered with the 6.5 meter Magellan Telescopes located at Las Campanas Observatory, Chile.
[1] Observatories of the Carnegie Institution of Washington, 813 Santa Barbara St., Pasadena, CA 91101, USA
[2] George P. and Cynthia Woods Mitchell Institute for Fundamental Physics and Astronomy, and Department of Physics and Astronomy, Texas A&M University, College Station, TX 77843, USA
[3] Fermi National Accelerator Laboratory, P. O. Box 500, Batavia, IL 60510, USA
[4] INAF- Osservatorio Astronomico di Torino - Strada Osservatorio 20, Pino Torinese, 10020, Italy
[5] ARC Centre of Excellence for All-Sky Astrophysics (CAASTRO)
[6] Department of Physics & Astronomy, University College London, Gower Street, London, WC1E 6BT, UK
[7] Department of Physics and Electronics, Rhodes University, PO Box 94, Grahamstown, 6140, South Africa
[8] LSST, 933 North Cherry Avenue, Tucson, AZ 85721, USA
[9] CNRS, UMR 7095, Institut d'Astrophysique de Paris, F-75014, Paris, France
[10] Sorbonne Universités, UPMC Univ Paris 06, UMR 7095, Institut d'Astrophysique de Paris, F-75014, Paris, France
[11] Laboratório Interinstitucional de e-Astronomia - LIneA, Rua Gal. José Cristino 77, Rio de Janeiro, RJ - 20921-400, Brazil
[12] Observatório Nacional, Rua Gal. José Cristino 77, Rio de Janeiro, RJ - 20921-400, Brazil
[13] Department of Astronomy, University of Illinois, 1002 W. Green Street, Urbana, IL 61801, USA
[14] National Center for Supercomputing Applications, 1205 West Clark St., Urbana, IL 61801, USA
[15] Institut de Ciències de l'Espai, IEEC-CSIC, Campus UAB, Carrer de Can Magrans, s/n, 08193 Bellaterra, Barcelona, Spain
[16] Institut de Física d'Altes Energies (IFAE), The Barcelona Institute of Science and Technology, Campus UAB, 08193 Bellaterra (Barcelona) Spain
[17] Kavli Institute for Particle Astrophysics & Cosmology, P.

O. Box 2450, Stanford University, Stanford, CA 94305, USA
[18] Department of Physics, IIT Hyderabad, Kandi, Telangana 502285, India
[19] Jet Propulsion Laboratory, California Institute of Technology, 4800 Oak Grove Dr., Pasadena, CA 91109, USA
[20] Kavli Institute for Cosmological Physics, University of Chicago, Chicago, IL 60637, USA
[21] Instituto de Fisica Teorica UAM/CSIC, Universidad Autonoma de Madrid, 28049 Madrid, Spain
[22] Department of Physics, University of Michigan, Ann Arbor, MI 48109, USA
[23] SLAC National Accelerator Laboratory, Menlo Park, CA 94025, USA
[24] Astronomy Department, University of Washington, Box 351580, Seattle, WA 98195, USA
[25] Cerro Tololo Inter-American Observatory, National Optical Astronomy Observatory, Casilla 603, La Serena, Chile
[26] Australian Astronomical Observatory, North Ryde, NSW 2113, Australia
[27] Institució Catalana de Recerca i Estudis Avançats, E-08010 Barcelona, Spain
[28] Department of Physics and Astronomy, Pevensey Building, University of Sussex, Brighton, BN1 9QH, UK
[29] Centro de Investigaciones Energéticas, Medioambientales y Tecnológicas (CIEMAT), Madrid, Spain
[30] Instituto de Física, UFRGS, Caixa Postal 15051, Porto Alegre, RS - 91501-970, Brazil
[31] Universidade Federal do ABC, Centro de Ciências Naturais e Humanas, Av. dos Estados, 5001, Santo André, SP, Brazil, 09210-580
[32] Computer Science and Mathematics Division, Oak Ridge National Laboratory, Oak Ridge, TN 37831

1. INTRODUCTION

A small fraction (∼5%) of metal-poor stars in the Milky Way (MW) halo show overabundances of elements produced by the rapid neutron-capture process (Barklem et al. 2005). These so-called r-process enhanced stars can be divided into two groups depending on their level of r-process enhancement: the r-I stars with $0.3 \lesssim$ [Eu/Fe] $\lesssim 1.0$ and the r-II stars with [Eu/Fe] > 1.0 (Beers & Christlieb 2005). It has long been recognized that the abundance pattern for the heavy neutron-capture elements in r-II stars follows the solar system r-process pattern (e.g., McWilliam et al. 1995; Hill et al. 2002; Sneden et al. 2003). The same was recently found to be true for the moderately enhanced and more numerous r-I stars (Siqueira Mello et al. 2014).

It has been suggested that r-process enhanced stars are the result of mass transfer from a binary companion (Qian & Wasserburg 2001). However, long term radial velocity monitoring performed by Hansen et al. (2011, 2015) of 17 r-process enhanced stars over a period of eight years showed that these stars have a binary frequency of ∼18%, consistent with the binary frequency for ordinary metal-poor field giants (Carney et al. 2003). Since many stars with r-process enhancements are therefore not in binaries, the unusual abundance patterns of the r-I and r-II stars must be the result of nucleosynthesis events in the early Universe. The suggested astrophysical sites for production of r-process elements include neutron star mergers (NSMs) (e.g., Lattimer & Schramm 1974; Meyer 1989; Freiburghaus et al. 1999; Metzger et al. 2010; Goriely et al. 2011; Korobkin et al. 2012; Bausswein et al. 2013; Rosswog et al. 2014) and various types of supernovae (SNe), including magneto-rotationally driven SNe (also known as jet SNe) (Cameron 2003; Fujimoto et al. 2008; Winteler et al. 2012) and neutrino-driven winds in core-collapse SNe (Arcones & Thielemann 2013, and references therein). The NSMs and jet SNe are referred to as main r-process sites and can produce the heavy r-process elements. The yields of the ejected material from these sites are predicted to match the Solar System's heavy r-process-element pattern (Fujimoto et al. 2008; Bausswein et al. 2013). Nucleosynthesis in neutrino driven winds in core-collapse SNe is referred to as the weak r-process and is thought to produce the lighter r-process elements up to $A \sim 100$ (Arcones et al. 2007).

In addition to their presence in the halo, a number of r-process enhanced stars have also been found in dwarf galaxies that are satellites of the Milky Way, highlighted by the discovery that seven of the nine brightest stars in the ultra-faint dwarf Reticulum II (Ret II) are r-II stars (Ji et al. 2016a; Roederer et al. 2016). Several long-studied dwarfs such as Draco, Ursa Minor (UMi), Sculptor, Fornax, and Carina also contain r-process enhanced stars (e.g., Cohen & Huang 2010; Tsujimoto et al. 2015; Lemasle et al. 2014; Shetrone et al. 2003), although the implications of these stars have received relatively little attention in the literature. These dwarf galaxies, including both the ultra-faint dwarfs and the classical dwarf spheroidals, provide a unique environment for exploring nucleosynthesis events in the early universe. Unlike stars from the Milky Way halo that may have been accreted by the Galaxy from a variety of smaller systems, the stars in dwarf galaxies are more likely to have remained in their birthplaces (Griffen et al. 2016). Hence, not only can the chemical abundances of the stars trace just a few nucleosynthesis events, but the galaxy as a whole also preserves a record of the environment in which the events occurred.

A large population of new Milky Way satellites, many of them quite nearby, has been identified over the past two years (e.g., Bechtol et al. 2015; Koposov et al. 2015; Drlica-Wagner et al. 2015), led by discoveries from the Dark Energy Survey (DES; The Dark Energy Survey Collaboration et al. 2016; Flaugher et al. 2015). One of the closest of these objects is Tucana III, located just 25 kpc away (Drlica-Wagner et al. 2015). Simon et al. (2016) presented spectroscopic confirmation of Tuc III and identified several bright member stars, including one star at $V = 15.8$ that is the brightest known star in an ultra-faint dwarf galaxy. This star, DES J235532.66−593114.9 (hereafter shortened to DES J235532), provides a unique opportunity to measure the abundance of heavy elements that ordinarily cannot be detected in the spectra of individual stars beyond the Milky Way.

In this paper, we present high-resolution Magellan/MIKE spectroscopy of DES J235532 and analyze its chemical abundance pattern. In §2 we briefly discuss our observations and data reduction. We describe our abundance analysis in §3. In §4 we compile a comparison sample of r-process enhanced stars in dwarf galaxies and in the Milky Way and examine the similarities between them. We consider the implications of these results for the chemical enrichment of Tuc III and r-process nucleosynthesis in dwarf galaxies in §5, and we present our conclusions in §6.

2. OBSERVATIONS

Simon et al. (2016) used medium-resolution spectroscopy to identify a sample of 26 member stars in Tuc III, including ten stars on the red giant branch that are brighter than $g \sim 20$. The color-magnitude diagram of Tuc III is displayed in Fig 1, and DES J235532 (shown as the green star) was selected as the brightest member of the system. The g and r magnitudes currently available from DES are calibrated at the 2% level and have statistical uncertainties ranging from 0.001 to 0.02 mag (Drlica-Wagner et al. 2015; Simon et al. 2016).

We observed DES J235532 with the MIKE spectrograph (Bernstein et al. 2003) on the Magellan/Clay telescope on the night of 2015 August 14. We obtained a total of 3.5 hr of integration time in generally poor seeing ($> 1''$), with some light cirrus present. The observations were made with a $1'' \times 5''$ slit, providing a spectral resolution of $R = 28000$ on the blue channel and $R = 22000$ on the red channel. We reduced the data with the latest version of the Carnegie MIKE pipeline originally described by Kelson (2003).[34] Because DES J235532 is so bright, the combined spectrum is of higher quality than most high-resolution spectra of stars in dwarf galaxies, reaching a S/N of ∼20 per pixel at 4100 Å, and ∼50 per pixel at 5500 Å.

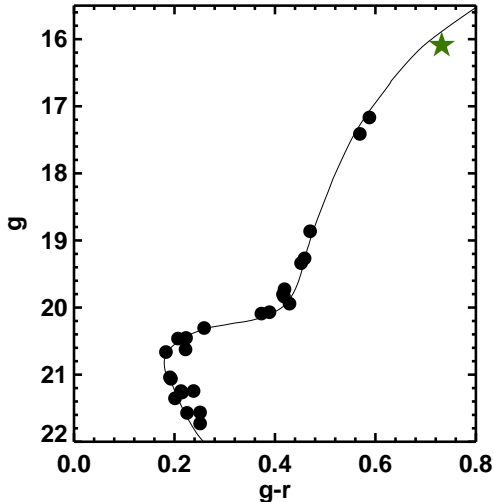[34] http://code.obs.carnegiescience.edu/mike

Figure 1. DES color-magnitude diagram for members of Tucana III from Simon et al. (2016). A Dartmouth isochrone (Dotter et al. 2008) for an age of 13 Gyr, [Fe/H] = −2.5 and [α/Fe] = 0.2 is overplotted (gray curve). DES J235532 is marked with a green star.

Table 1
Fe I and Fe II lines used for parameter determination.

Species	λ (Å)	χ (eV)	log gf (dex)	EW (mÅ)	log ϵ (dex)
Fe I	3743.36	0.99	-0.785	215.5	5.29
Fe I	3787.88	1.01	-0.859	177.6	5.03
Fe I	3849.97	1.01	-0.871	202.6	5.27
Fe I	3865.52	1.01	-0.982	163.1	4.93
Fe I	3917.18	0.99	-2.155	121.6	5.24
Fe I	3949.95	2.18	-1.251	98.0	5.21
Fe I	4076.63	3.21	-0.529	64.3	4.99
Fe I	4114.44	2.83	-1.303	52.2	5.11
Fe I	4132.06	1.61	-0.675	170.0	5.32
Fe I	4132.90	2.85	-1.006	57.8	4.92
.	.	.	.	.	.
.	.	.	.	.	.
Fe II	4416.82	2.78	-2.410	61.2	4.93
Fe II	4489.18	2.83	-2.971	34.6	5.09
Fe II	4508.28	2.86	-2.250	71.9	5.04
Fe II	4515.33	2.84	-2.450	63.2	5.07

Note. — The complete version of Table 1 is available online only. A short version is shown here to illustrate its form and content.

3. STELLAR PARAMETER MEASUREMENTS AND ABUNDANCE ANALYSIS

Stellar parameters for DES J235532 have been determined from equivalent width measurements of 120 Fe I and 25 Fe II lines listed in Table 1. The effective temperature ($T_{\rm eff}$) was derived from excitation equilibrium and then corrected for the offset between spectroscopic and photometric temperature scales using the method of Frebel et al. (2013). The surface gravity was determined by ensuring abundance agreement between Fe I and Fe II lines, and the microturbulence was calculated by eliminating any abundance trend with reduced equivalent width for both Fe I and Fe II lines. The final parameters are listed in Table 3. By varying the temperature and evaluating the resultant trend of the abundances with excitation potential we estimate the uncertainty of $T_{\rm eff}$ to be 100 K. The standard deviation of the Fe I abundances is 0.18 dex, calculated from the 120 Fe I lines used for parameter determination. Based on this value and the uncertainty in $T_{\rm eff}$ we estimate uncertainties of 0.3 dex for log$g$ and 0.3 km s^{-1} for the microturbulence. We have used a spectrum of Arcturus to check our line list and find good agreement with the parameters derived by Ramírez et al. (2013). The velocity of DES J235532 was measured by cross-correlating each order of the spectrum with a high S/N MIKE spectrum of the bright, metal-poor giant HD 122563, assuming a velocity of $v_{\rm hel} = -26.51$ km s^{-1} for HD 122563 (Chubak et al. 2012). The MIKE velocity of DES J235532 is in good agreement with the average velocity for the star of $v_{hel} = -103.2 \pm 1.2$ km s^{-1} measured by Simon et al. (2016) from two medium-resolution spectra, as well as with the mean radial velocity of $v_{hel} = -102.4$ km s^{-1} found by Simon et al. for 26 member stars of Tuc III.

The abundances have been derived via spectrum synthesis using the 2011 version of the LTE spectral synthesis program MOOG (Sneden 1973), which includes proper treatment of continuum scattering (Sobeck et al. 2011). We used an α-enhanced [α/Fe] = 0.4 ATLAS9

model atmosphere (Castelli & Kurucz 2003). The cool temperature of this star along with its carbon and iron abundances ([C/Fe] = −0.25 and [Fe/H] = −2.25) results in many of the absorption lines being blended, mainly due to the presence of many molecular CH lines in the spectrum, hence an abundance analysis including all elements detected in the spectrum can only be done with spectrum synthesis. Excitation potentials and oscillator strengths for the lines employed are taken from the VALD database (Ryabchikova et al. 2015), except for Ba where values from Fuhr & Wiese (2009) were used. For lines exhibiting isotopic shifts and/or hyperfine splitting (Sc, Mn, Co, Cu, Ba, La, Pr, Nd, Sm, Eu and Er) the isotope ratios and hyperfine structure collected by Roederer et al. (2014a) were used. Lines used in the abundance analysis are listed in Table 2. Molecular line lists for CH, NH and CN are from Masseron et al. (2014) and T. Masseron (private comm.), assuming dissociation energies of 3.47 eV, 3.42 eV and 7.74 eV for the species CH, NH and CN respectively. The C abundance was determined from the CH G-band at 4300 Å and the N abundance from the CN band at 3890 Å assuming an oxygen abundance of [O/Fe] = 0.4. We use solar abundances from Asplund et al. (2009). Figure 2 shows portions of the spectrum of DES J235532 along with syntheses of the most prominent lines of three r-process elements: Pr (λ4179 Å), Sm (λ4467 Å), and Eu (λ4129 Å).

4. RESULTS

4.1. *Abundance Pattern of DES J235532*

We have derived abundances or useful upper limits for 30 elements in DES J235532, including 13 neutron-capture species. Final abundances with uncertainties arising from stellar parameter uncertainties, line information, and continuum placement are listed in Table 3. Uncertainties from stellar parameters were computed by deriving abundances with different atmosphere models, each with one parameter varied by its uncertainty as quoted in §3. These uncertainties were then added in
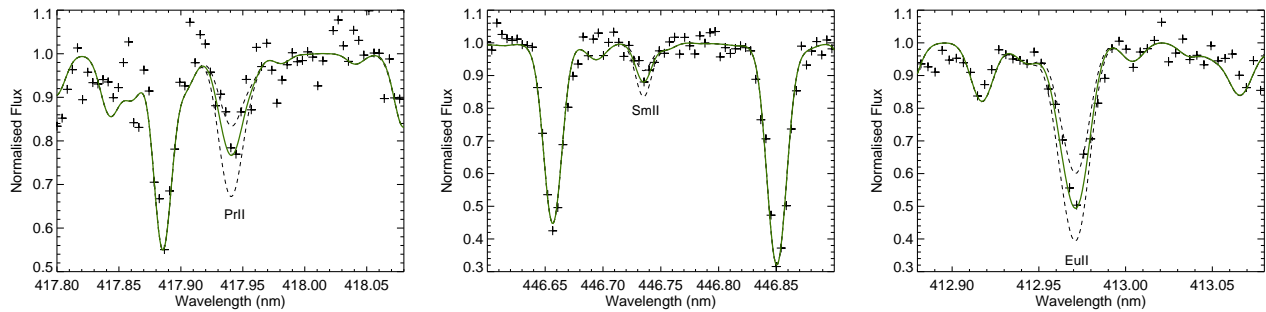
Figure 2. Spectrum synthesis of the r-process elements Pr (left), Sm (middle) and Eu (right) in DES J235532. The green solid lines show the spectrum fit and dashed lines show $[X/Fe] \pm \sigma_{[X/Fe]}$

Table 2
Atomic line data.

Species	λ (Å)	χ (eV)	$\log gf$ (dex)
O I	6300.30	0.00	-9.78
Na I	5889.95	0.00	0.11
Na I	5895.92	0.00	-0.19
Mg I	3829.36	2.71	-0.21
Mg I	3832.30	2.71	0.13
Mg I	3838.29	2.72	0.40
Mg I	4167.27	4.35	-0.71
Mg I	5172.68	2.71	-0.45
Mg I	5183.60	2.72	-0.24
Mg I	5528.40	4.34	-0.50
Al I	3944.00	0.00	-0.64
Si I	3905.52	1.91	-1.04
Si I	4102.94	1.91	-3.14

Note. — The complete version of Table 2 is available online only. A short version is shown here to illustrate its form and content.

Table 3
Stellar Parameters and Derived
Abundances for DES J235532

RA	23:55:32.8
Dec	-59:31:12.0
v_{hel} ($\pm$0.3 km s^{-1})	-103.4

Parameters	
T_{eff} ($\pm$100 K)	4720
$\log g$ ($\pm$0.3 dex)	1.33
[Fe/H] ($\pm$0.18 dex)	-2.25
ξ ($\pm$0.3 km s^{-1})	2.0

Abundances [X/Fe]	
C	-0.25 (0.25)
N	$+0.10$ (0.26)
O	$<+0.40$ $\cdots$
Na	$+0.19$ (0.30)
Mg	$+0.39$ (0.29)
Al	-0.86 (0.30)
Si	$+0.52$ (0.31)
K	$+0.29$ (0.19)
Ca	$+0.05$ (0.20)
Sc	$+0.01$ (0.29)
Ti	$+0.10$ (0.28)
Cr	-0.45 (0.19)
Mn	-0.57 (0.25)
Co	$+0.13$ (0.27)
Ni	-0.09 (0.22)
Cu	<-0.60 $\cdots$
Zn	-0.02 (0.18)
Sr	-0.39 (0.27)
Y	-0.44 (0.18)
Zr	$+0.05$ (0.21)
Ba	-0.16 (0.18)
La	$+0.04$ (0.20)
Ce	-0.19 (0.17)
Pr	$+0.56$ (0.23)
Nd	$+0.21$ (0.23)
Sm	$+0.56$ (0.18)
Eu	$+0.60$ (0.19)
Gd	$+0.53$ (0.20)
Dy	$+0.65$ (0.21)
Er	$+0.61$ (0.23)

quadrature to the estimated 0.1 dex uncertainty from line information and continuum placement. DES J235532 exhibits a clear enhancement in Europium ([Eu/Fe] = 0.60) and other neutron-capture elements primarily produced in the r-process and can therefore be classified as an r-I star.

Apart from neutron-capture species, the abundances of DES J235532 are generally unremarkable. Its metallicity of [Fe/H] = -2.25 places it slightly above the mean metallicity of Tuc III, and is consistent within the uncertainties with the value calculated by Simon et al. (2016) using the Ca triplet method. The α elements in DES J235532 are enhanced relative to solar ratios, as expected for its metallicity, with the possible exception of a moderately low Ca abundance ([Ca/Fe] is consistent with a normal enhancement within the uncertainties). DES J235532 is not enhanced in carbon.

The nature of Tuc III was discussed by Simon et al. (2016), who suggested that the system is most likely a dwarf galaxy, although they could not definitively rule out a globular cluster classification. The abundance pattern of the stars in Tuc III could potentially provide additional insight into this question. However, with only one star we can not determine whether Tuc III contains the typical light element abundance correlations seen in cluster stars. We note that r-process enhanced stars have been found in both clusters and in dwarf galaxies (Roederer et al. 2011; Yong et al. 2013). For the remain-

der of this paper we assume that Tuc III is a dwarf galaxy, as favored by the evidence presented by Simon et al. (2016).

4.2. r-process Enhanced Stars in Dwarf Galaxies

As mentioned in §1, a number of r-process enhanced stars have been found in other dwarf galaxies, namely in the classical dwarf spheroidals (dSphs) UMi, Draco,

Sculptor, Fornax, and Carina, as well as Ret II. No r-process enhanced stars in ultra-faint dwarfs were known prior to the discovery of Ret II; François et al. (2016) found a few stars in Hercules, Canes Venatici I, and Canes Venatici II with high Sr and/or Ba abundances, but without measurements of other neutron-capture elements it is not clear whether these stars were enriched by the r-process or the s-process.

To provide a comparison set for DES J235532, in this section we compile a sample of all known r-process enhanced stars in dwarf galaxies from the literature. Our selection criteria, which will be explored further in §4.3, are [Eu/Fe] > 0.3 and [Eu/Ba] > 0.4. In the following, we examine Eu measurements for stars in the individual galaxies. The final selected r-I (0.3 < [Eu/Fe] < 1.0) and r-II ([Eu/Fe] > 1.0) stars are listed in Tables 4 and 5, respectively.

Ursa Minor

In UMi, 17 giant stars have been analysed with high resolution spectroscopy (Shetrone et al. 2001; Sadakane et al. 2004; Cohen & Huang 2010; Kirby & Cohen 2012). Of the ten stars in the sample of Cohen & Huang (2010), five can be labeled as r-I stars. Four of the remaining stars have subsolar Eu abundances, while for one only an upper limit is available. All stars in this sample with measured Eu have lower Ba abundance than Eu abundance. One r-I star and one r-II star were found among the six stars studied by Shetrone et al. (2001). Additionally, two other stars from Shetrone et al. (2001) show [Eu/Fe] = 0.26 ± 0.2 and 0.15 ± 0.20, consistent with a solar [Eu/Fe] ratio or a slight Eu enhancement, and a third has [Eu/Fe] = 1.04 while also having [Ba/Fe] = 1.37. The [Ba/Fe] ratios range from −0.39 to 1.37, but aside from the star with highest Ba abundance, all have higher Eu abundances. Two of the three stars studied by Sadakane et al. (2004) overlap with the sample of Shetrone et al. (2001) and were already identified as r-process enhanced there. For the third star they find [Ba/Fe] = −1.28, but no Eu abundance is given. Finally, Kirby & Cohen (2012) find [Ba/Fe] = −0.93 and an upper limit of [Eu/Fe] < 0.23 for the one UMi star they observed. Hence of the 17 UMi stars for which Eu measurements are available, ten have super-solar r-process abundance ratios ([r/Fe] > 0) and seven qualify as r-I or r-II stars.

Draco

For the Draco dSph, six giants were analysed by Shetrone et al. (2001), who found two r-I stars, and a further eight stars were studied by Cohen & Huang (2009), including two additional r-I stars, one r-II star, and one star with [Eu/Fe] = 0.19 ± 0.19. Of the six stars analysed in Shetrone et al. (2001), [Ba/Fe] ratios were derived for five, ranging from −1.19 to 0.41, with the two r-I stars at [Ba/Fe] = 0.11 and 0.09. Ba abundances were derived for all eight stars studied by Cohen & Huang (2009), with the majority having subsolar Ba abundances. The r-II star with [Ba/Fe] = 0.26 shows the highest Ba abundance in the sample. Tsujimoto et al. (2015) also analysed three stars in Draco and found one star with a small Eu enhancement of 0.12 dex and [Ba/Fe] = −0.69. Therefore, seven of the 17 stars in Draco with high

resolution spectra in the literature are enhanced in r-process elements, with five qualifying as r-I or r-II stars. For the remaining ten objects, two have upper limits of [Eu/Fe] < 0.12 and 0.41, while eight stars have no Eu abundance measured.

Sculptor

Seven papers report Eu abundances or upper limits for a total of 21 stars in Sculptor (Shetrone et al. 2003; Geisler et al. 2005; Tafelmeyer et al. 2010; Kirby & Cohen 2012; Simon et al. 2015; Jablonka et al. 2015; Skúladóttir et al. 2015). Eight of these stars show enhancement in r-process elements, including one r-I star from the sample of Kirby & Cohen (2012). The other seven stars with Eu enhancement (four from Shetrone et al. 2003 and three from Geisler et al. 2005) are also enhanced in the s-process element Ba. Of the remaining 13 stars, three have subsolar Eu detection or upper limits (Geisler et al. 2005; Jablonka et al. 2015), nine have upper limits above solar that do not provide significant constraints (Tafelmeyer et al. 2010; Simon et al. 2015; Jablonka et al. 2015), and one is identified as a CEMP-no star[35] (Skúladóttir et al. 2015). In summary only one of the 21 stars in Sculptor with Eu measurements qualifies as an r-I star and none are r-II stars.

Fornax

The dSph Fornax is well studied, with neutron-capture element abundances published for 147 stars (Shetrone et al. 2003; Tafelmeyer et al. 2010; Letarte et al. 2010; Lemasle et al. 2014). The majority of these are enhanced not only in Eu but also in s-process elements such as Ba and La, such that only six qualify as r-I stars; three from the sample of Lemasle et al. (2014) and three from the sample of Letarte et al. (2010). Furthermore one star from Lemasle et al. (2014) and three stars from Letarte et al. (2010) qualify as r-II stars, resulting in a total of 10 r-I and r-II stars discovered in this galaxy.

Carina

Shetrone et al. (2003) and Venn et al. (2012) have published Eu abundances or upper limits for five and nine stars, respectively, in the Carina dSph. Here two stars qualify as r-I stars, one from each sample, while the rest either show a similar enhancement in s-process elements or only have an upper limit on the Eu abundance.

Reticulum II

Nine stars in Ret II have been analysed with high resolution spectroscopy, and seven of these show large enhancements in r-process elements (Ji et al. 2016a,b; Roederer et al. 2016). One of the r-process enhanced stars in Ret II also has a high Ba abundance ([Eu/Ba] = 0.3) and does not meet our selection criteria. The remaining six stars are listed in Table 5.

A number of r-process enhanced stars in the halo also show enhancements in carbon (e.g., CS 22892−052; Sneden et al. 2003) and overall carbon enhancement is the most common abundance peculiarity in metal-poor

---

[35] Carbon enhanced metal-poor star with no enhancement in neutron-capture elements (Beers & Christlieb 2005).

stars. All of the stars listed in Table 3 and 4 are evolved giants and thus some change in their original carbon abundances is expected from stellar evolution. We have performed carbon corrections using the tool provided by Placco et al. (2014) but even though corrections are substantial ($\sim 0.6 - 0.7$ dex), none of the r-I or r-II stars in UMi, Draco, or Sculptor qualify as being carbon-enhanced metal-poor stars (CEMP; [C/Fe] ≥ 0.7; Aoki et al. 2007). For the six Fornax and two Carina stars, no C abundances are available. Ji et al. (2016b) performed the same exercise for the r-process enhanced stars in Ret II and found three of them to be carbon enhanced.

4.3. Pollution From s-process Nucleosynthesis

Europium is mainly produced in the r-process, while Barium is mainly produced in the s-process in asymptotic giant branch (AGB) stars, so the ratio of the two is a diagnostic of the onset of the s-process, seen as a decline in the [Eu/Ba] ratio with increasing metallicity. Simmerer et al. (2004) found an r-process ratio of [Eu/Ba] = 0.70 for the Solar System. The two classic halo r-II stars CS 31082−001 (Siqueira Mello et al. 2013) and CS 22892−052 (Roederer et al. 2014a), which are often used as templates of the r-II abundance pattern, have slightly lower abundance ratios of [Eu/Ba] = 0.53 and [Eu/Ba] = 0.41, respectively. Based on these measurements we included a limit on the [Eu/Ba] ratio of [Eu/Ba] > 0.4 to ensure that the heavy element abundance patterns of the neutron-capture-enhanced stars selected in §4.2 are dominated by the r-process contribution and have not been severely polluted by s-process material. [Eu/Ba] ratios for all of the selected r-I and r-II stars are listed in Tables 4 and 5. For DES J235532 we find [Eu/Ba] = 0.76, similar to what is found for the r-I and r-II stars in the other dwarfs.

Kirby & Cohen (2012) detected no decline in the [Eu/Ba] ratio with increasing metallicity in UMi after combining the samples of Shetrone et al. (2001); Sadakane et al. (2004) and Cohen & Huang (2010). The authors suggest that the [Eu/Ba] ratio is constant because star formation in UMi had stopped by the time that its AGB stars began to pollute the ISM, so the s-process elements created there were never incorporated into any new stars. However, we note that (as mentioned above) one UMi star with [Fe/H] = −2.17, from the sample of Shetrone et al. (2003), does show a large enhancement in Ba in addition to its Eu enhancement. Also, the six r-I stars in UMi listed in Table 4 do show a small decline in [Eu/Ba] with increasing metallicity.

In Fornax and Sculptor, on the other hand, the [Eu/Ba] ratio starts to decline at [Fe/H] = −1.5 (Lemasle et al. 2014) and [Fe/H] $\sim$ −1.8 (Kirby & Cohen 2012), respectively, and Cohen & Huang (2009) detect a decline at similar metallicity in Draco. The majority of our selected r-I stars have metallicities similar to or lower than these values, supporting the idea that the neutron-capture elements in these stars were primarily produced by the r-process.

4.4. r-I Abundance Pattern in Dwarf Galaxies

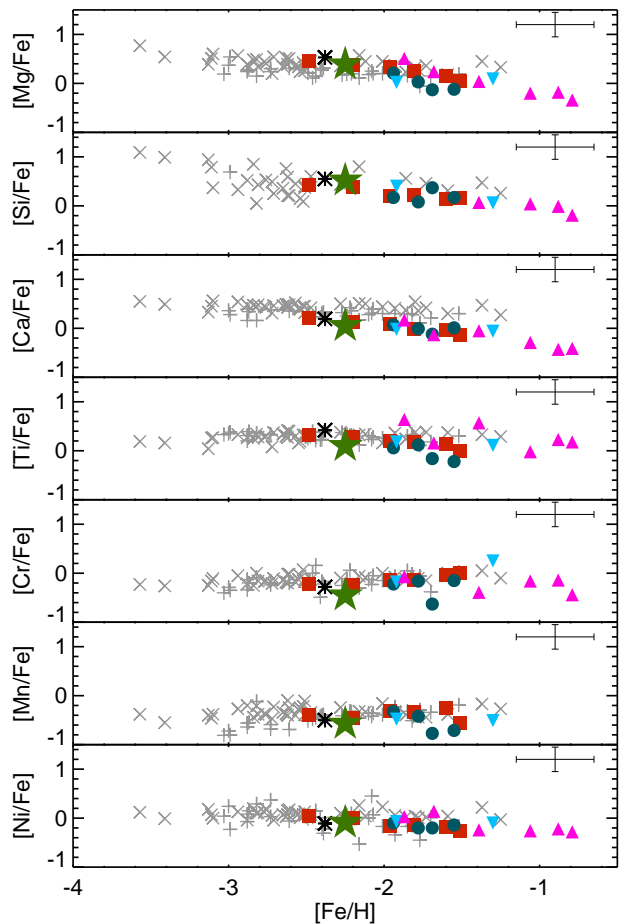To constrain the origin of metal-poor r-process enhanced stars, in this subsection we compare their abun-

Figure 3. Mg, Si, Ca, Ti, Cr, Mn and Ni abundances for r-I stars in dwarf galaxies and in the halo. A typical error bar is displayed in the upper right corner of each panel. The plotted sample includes Tuc III (green star), UMi (red squares), Draco (dark blue circles), Sculptor (black asterisks), Carina (light blue upside-down triangles), Fornax (magenta triangles), and halo stars (grey plusses from Barklem et al. 2005 and crosses from Roederer et al. 2014a). References for literature dwarf galaxy data are given in Table 3.

dance patterns to those of ordinary metal-poor halo stars and to the r-process abundance pattern found in the Sun.

4.4.1. Light elements

Siqueira Mello et al. (2014) and Roederer et al. (2014b) explored abundances for the light elements from Mg to Ni in r-I and r-II stars (respectively) and found no significant difference between the abundances in r-process enhanced stars and normal halo stars.

Figure 3 shows the abundances for the α and iron peak elements in DES J235532 compared with r-I stars from the halo (Roederer et al. 2014a; Barklem et al. 2005) and r-I stars from UMi, Draco, Sculptor, Fornax and Carina. All abundances have been converted to the Asplund et al. (2009) solar abundance scale. For the majority of the α and iron peak elements, similar abundances are found in the halo r-I and dwarf galaxy r-I stars. The possible exception is Ca, where as noted in §4.1, DES J235532 has a slightly lower abundance than most halo stars at similar metallicity. The other

Table 4
[Fe/H], [Eu/Fe] and [Eu/Ba] ratios for *r*-I stars identified in dwarf galaxies.

Star ID	[Fe/H]	[Eu/Fe]	[Eu/Ba]	Ref
		Tuc III		
DES J235532	-2.25	0.60	0.76	This paper
		UMi		
N37	-1.55	0.87	0.68	Cohen & Huang (2010)
J12	-1.76	0.83	0.56	Cohen & Huang (2010)
297	-1.68	0.74	0.59	Shetrone et al. (2001)
27940	-1.91	0.61	0.66	Cohen & Huang (2010)
COS233	-2.15	0.52	0.70	Cohen & Huang (2010)
36886	-2.43	0.44	0.79	Cohen & Huang (2010)
		Draco		
3150	-1.89	0.84	0.70	Cohen & Huang (2009)
11	-1.72	0.55	0.48	Shetrone et al. (2001)
343	-1.86	0.51	0.45	Shetrone et al. (2001)
3053	-1.73	0.39	0.54	Cohen & Huang (2009)
		Sculptor		
1019417	-2.45	0.39	0.83	Kirby & Cohen (2012)
		Fornax		
mem0612	-1.68	0.93	1.22	Lemasle et al. (2014)
rgb 0522	-1.87	0.76	1.11	Lemasle et al. (2014)
mem0747	-1.39	0.68	0.67	Lemasle et al. (2014)
BL196	-1.06	0.59	0.42	Letarte et al. (2010)
BL190	-0.79	0.54	0.48	Letarte et al. (2010)
BL228	-0.88	0.41	0.46	Letarte et al. (2010)
		Carina		
Car 10	-1.94	0.80	0.55	Shetrone et al. (2003)
1013	-1.30	0.33	0.48	Venn et al. (2012)

Table 5
[Fe/H], [Eu/Fe] and [Eu/Ba] ratios for *r*-II stars identified in dwarf galaxies.

Star ID	[Fe/H]	[Eu/Fe]	[Eu/Ba]	Ref
		UMi		
199	-1.45	1.49	0.72	Shetrone et al. (2001)
		Draco		
21456	-2.34	1.05	0.79	Cohen & Huang (2009)
		Fornax		
BL147	-1.38	1.72	0.43	Letarte et al. (2010)
BL204	-1.00	1.26	0.80	Letarte et al. (2010)
BL311	-0.78	1.24	0.61	Letarte et al. (2010)
mem0704	-2.55	1.10	0.70	Lemasle et al. (2014)
		Reticulum II		
DES J033454-540558	-2.77	2.11	0.71	Ji et al. (2016b)
DES J033447-540525	-2.91	1.86	0.78	Ji et al. (2016b)
DES J033457-540531	-2.08	1.76	0.40	Ji et al. (2016b)
DES J033607-540235	-2.97	1.74	0.83	Ji et al. (2016b)
DES J033523-540407	-3.01	1.68	0.89	Ji et al. (2016b)
DES J033548-540349	-2.19	0.95	0.59	Ji et al. (2016b)

dwarf galaxy r-I stars also have on average $\sim$0.2 dex
lower [Ca/Fe] abundances than the halo r-I stars. A
similar trend may be seen at higher metallicities for Ti
with lower significance. It should be noted, though, that
the r-process enhanced stars in the halo cover a wider
metallicity range than those in dwarf galaxies, with the
majority having [Fe/H] < -2.5, mainly due to selection
effects in halo surveys, while the dwarf galaxy stars are
all at [Fe/H] > -2.5. Thus, it would be interesting to ex-
amine a larger sample of higher-metallicity halo r-I stars
to see if their Ca and Ti abundances are indeed distinct
from the dwarf galaxy r-I stars.

4.4.2. *Neutron-capture elements*

It was recognized from early on that for the highly
r-process enhanced r-II stars in the halo the heavy
neutron-capture element ($Z \geq 56$) abundance ratios
match those of the Solar System (McWilliam et al. 1995;
Barklem et al. 2005). Recently this result was found
to extend to dwarf galaxy stars when Ji et al. (2016a)
and Roederer et al. (2016) found an equally good match
for the r-II stars discovered in Ret II. Furthermore,
Siqueira Mello et al. (2014) compared the abundance
pattern from Sr to Th of halo r-I stars to that of the
halo r-II star CS 31082$-$001, finding good agreement for
the heavy elements (Ba to Th), while the light neutron-
capture elements Sr, Y, and Zr were more enhanced in
the r-I stars relative to CS 31082$-$001. Thus the heavy
neutron-capture element abundance pattern seen in all
r-process enhanced stars in the halo and Ret II matches
that of the Solar System.

In Figure 4 we compare the neutron-capture ele-
ment absolute abundance pattern for the r-I stars de-
tected in the aforementioned dwarf galaxies, along with
DES J235532, with the abundance pattern of the clas-
sical r-II star CS 22892$-$052 taken from Sneden et al.
(2003), normalized to the Eu abundance. Also shown
is a difference plot with the stellar abundance differ-
ences between the individual dwarf galaxy stars and
CS 22892$-$052. The abundance uncertainties are com-
parable to the height of the plotted symbols. For the
Sculptor r-I stars only upper limits were reported for
the heavy neutron-capture elements besides Eu and Ba,
making it difficult to determine whether the abundance
pattern follows that of CS 22892$-$052, hence these stars
have not been included in Figure 4. The same is also
the case for three of the six r-I stars in Fornax, there-
fore only BL190, BL196, and BL228 have been included.
For the remainder, abundances have been reported for
four or more elements. As can be seen there is good
overall agreement for the heavy elements between the
abundance pattern of CS 22892$-$052 and the abundance
patterns of the r-process enhanced stars found in dwarf
galaxies, with an average abundance difference of only
0.16 dex for the elements from Ba to Er. In particular,
the result of Siqueira Mello et al. (2014) for the r-I stars
in the halo — that the abundance pattern follows the
same r-process pattern as the r-II stars — is also valid
for r-I stars in dwarf galaxies.

4.5. *Source of r-Process Enrichment in Dwarf Galaxies*

Tsujimoto & Shigeyama (2014) examined literature
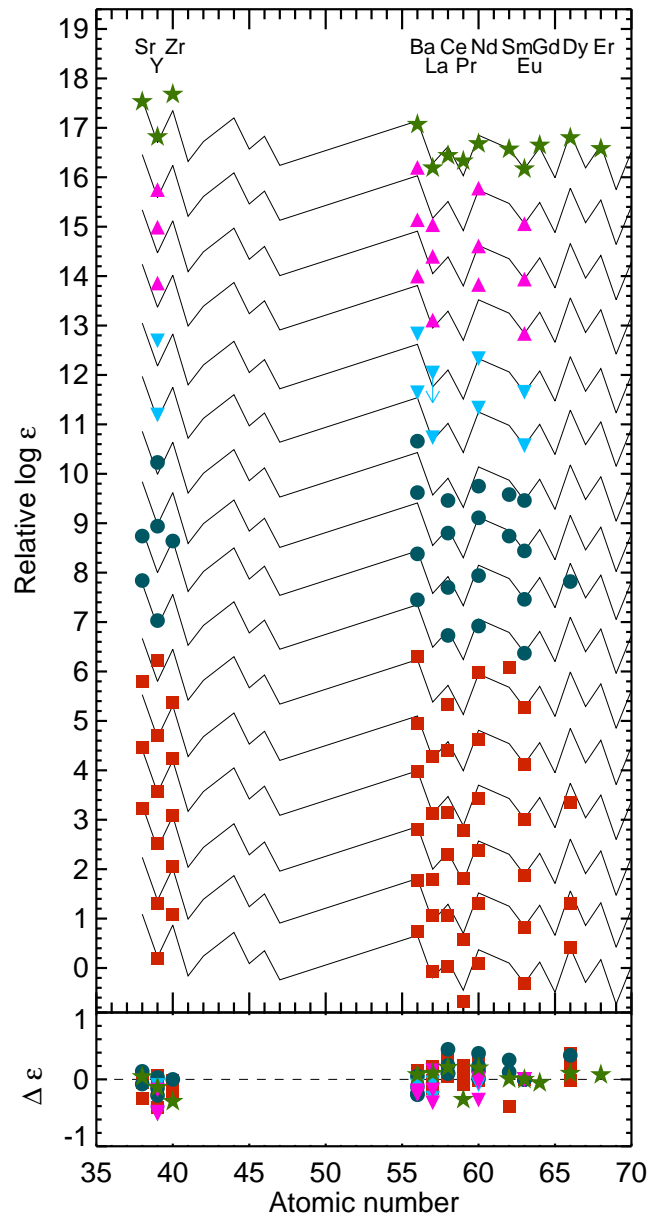data for Eu abundances for stars in a number of dwarf

Figure 4. Scaled neutron-capture element abundances for
dwarf galaxy r-I stars compared to the abundance pattern of
CS 22892$-$052 (solid line). The bottom panel shows the individual
stellar abundance offsets with respect to CS 22892$-$052 after nor-
malizing to the Eu abundance. The green stars show the derived
abundances for DES J235532 in Tuc III from this paper. Stars
in other dwarf galaxies from the literature are plotted as magenta
triangles (Fornax), light blue upside-down triangles (Carina), dark
blue circles (Draco), and red squares (UMi). References for the lit-
erature data are given in Table 3. The height of the plotted points
is representative of the abundance uncertainties and the arrow for
the first Carina star indicates an upper limit.

galaxies (Carina, Draco, Sculptor, Fornax, Sagittarius [Sgr], Ursa Major II, Hercules, and Coma Berenices) and found different behavior for this element between the various galaxies. Some systems exhibit a constant Eu level of [Eu/H] ~ -1.3 over the metallicity range ($-2 \lesssim$ [Fe/H] $\lesssim -1$), while others show a steady increase in Eu with metallicity. The authors argue that this result can be explained if the r-process enrichment is due to NSMs, where the galaxies showing a plateau have on average experienced < 0.1 NSM and were enriched by gas from a more massive neighbor, while galaxies with an increasing trend in Eu with Fe have hosted multiple NSMs. Carina and Sculptor are examples of the galaxies with apparent Eu plateaus. Larger galaxies such as Fornax and Sgr are examples of the latter (no Eu plateau with increasing metallicity), probably because their stellar masses are large enough that multiple NSMs are likely to have occurred. Draco, which has a smaller stellar mass, contains low metallicity stars with very low Eu abundance, such as Draco 119 with [Eu/H] < -2.55 (Fulbright et al. 2004). Tsujimoto et al. (2015) derived Eu abundances for two additional stars in Draco. In combination with the literature sample, these data suggest that stars with [Fe/H] < -2.2 have no Eu enrichment, followed by a sudden increase of 0.7 dex in the Eu abundance for stars with [Fe/H] > -2.2. This pattern led Tsujimoto et al. (2015) to reject the theory of pre-enrichment for Draco and suggest that a NSM occurred in the galaxy once its metallicity reached [Fe/H] ~ -2.2, although that hypothesis may not be consistent with Draco's gas accretion history (Ji et al. 2016a).

In Figure 5 we plot the [Eu/H] ratios (left) and the [Eu/Fe] ratios (right) as a function of metallicity for the r-I and r-II stars compiled in §4.2 along with the r-II stars found in Ret II and the r-I star presented in this paper; the right plot also shows the distribution of [Eu/Fe] ratios. Most strikingly, the stars in the low mass galaxy Ret II (green diamonds) show a clear increase in Eu with Fe. A similar trend is seen for the stars in UMi (red squares), with a stellar mass two orders of magnitude higher (and a comparable mass to Draco). These two galaxies also follow the general trend of [Eu/H] for r-process enhanced stars in the halo. DES J235532 (green star) has a [Eu/H] ratio placing it in the middle of the halo stars and at the lower end of the dwarf galaxy stars. With the expanded sample of stars from Tables 3 and 4 the low-metallicity plateau at [Eu/H] ~ -1.3 seen by Tsujimoto & Shigeyama (2014) for the low luminosity systems is no longer apparent.

Based on the increase seen in [Eu/H] with [Fe/H] in Fornax and Sgr, Tsujimoto & Shigeyama (2014) conclude that more than one NSM must have occurred in these galaxies. However, the data for Ret II indicate that the same signature can be produced with inhomogeneous mixing and a single NSM (Ji et al. 2016a). Also, Fornax and Sgr have both been found to be enriched in s-process elements, potentially providing an alternative source for the additional Eu observed in their higher metallicity stars (McWilliam et al. 2013; Letarte et al. 2010), hence the Eu abundances is not necessarily a clean tracer of the r-process in these galaxies.

5. DISCUSSION

The overall good agreement between the heavy element abundance patterns of DES J235532, of r-I stars from other dwarf galaxies, and that of CS 22892−052, along with the similarly good agreement found when comparing the r-II stars in Ret II to CS 22892−052 (Ji et al. 2016b; Roederer et al. 2016), suggests a common astrophysical source for the r-process elements in r-I and r-II stars in both the halo and dwarf galaxies. As argued by Ji et al. (2016a), this source must be rare and each event must produce large quantities of r-process material ($\sim 10^{-4.5}$ M$_\odot$ of Eu), which is best explained by a NSM or magneto-rotationally driven SN.

The detection of an r-I star in the ultra-faint dwarf galaxy Tuc III raises several questions. If r-process nucleosynthesis events are rare, how did a galaxy as small as Tuc III become enhanced in such elements? And why does it have an r-I star with moderate r-process enhancement, in contrast to Ret II, whose r-process enhanced stars are all extremely-enhanced r-II stars?

We explore two possible scenarios for the r-process enrichment of Tuc III. Tsujimoto & Shigeyama (2014) pointed out that because of the high ejecta velocities from neutron star mergers, the r-process material they synthesize can spread into large volumes with stopping lengths that exceed the radii of dwarf galaxies. Furthermore, Komiya & Shigeyama (2016) show that a significant fraction of the NSM ejecta can escape the proto-galaxies entirely, polluting the surrounding intergalactic medium (IGM) and other nearby proto-galaxies. If Tuc III formed near other systems, perhaps it was polluted by ejecta from a NSM in a larger nearby galaxy. On the other hand, if a NSM occurred in Tuc III itself, depending on its gas distribution at the time and the geometry of the explosion, much of the resulting r-process debris could have escaped from the system, producing a lower level of enrichment than in Ret II. Future analysis of a larger sample of stars in Tuc III will reveal whether the galaxy has an overall enhancement of r-process elements seen in many stars, or if DES J235532 is an outlier.

Alternatively, we note that the r-I stars drawn from the literature have mostly been identified in more luminous dwarf galaxies. These systems likely had larger gas reservoirs at early times into which the ejecta from an r-process event could be diluted. The observed spread of r-process abundances within these galaxies, including both r-I and r-II stars, may have resulted from incomplete or inhomogeneous mixing. With a stellar mass of M$_* = 800$ M$_\odot$ (Drlica-Wagner et al. 2015), Tuc III is the lowest-luminosity dwarf found to contain an r-I star. However, there is evidence that Tuc III was more massive in the past. Drlica-Wagner et al. (2015) discovered apparent tidal tails on either side of the galaxy (see their Fig. 8). The integrated luminosity of the tails is comparable to the current luminosity of Tuc III itself, suggesting that at least half of the stellar mass has been lost to tidal stripping. With current data it is difficult to place an upper limit on the amount of mass that could have been stripped. According to the tidal evolution models of Peñarrubia et al. (2008), the current luminosity and velocity dispersion of Tuc III are consistent with the stripping of a $\sim 10^6$ L$_\odot$ progenitor similar to the classical dSphs (Simon et al. 2016), but that would imply the loss of 99.9% of its initial stellar mass. Deeper imaging of the tails of Tuc III and a proper motion measurement to de-
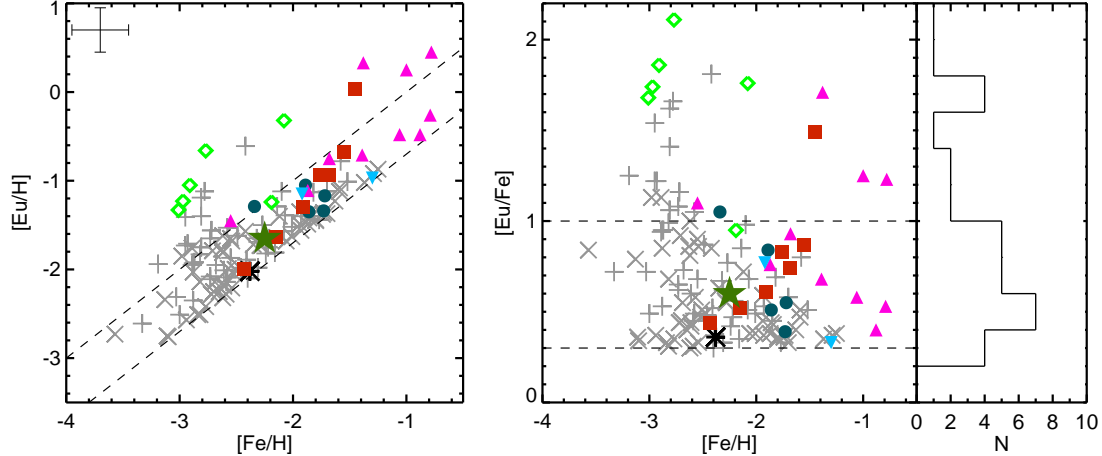
Figure 5. [Eu/H] abundances (left) and [Eu/Fe] abundances and distribution (right) for r-I and r-II stars in dwarf galaxies and in the halo. The [Eu/Fe] histogram in the right panel only includes stars in dwarf galaxies. The plotted sample includes Tuc III (green star), UMi (red squares), Draco (dark blue circles), Sculptor (black asterisks), Carina (light blue upside-down triangles), Fornax (magenta triangles), and Ret II (light green diamonds; Ji et al. 2016b). The halo stars shown here are taken from Barklem et al. (2005, grey plusses) and Roederer et al. (2014a, grey crosses). References for literature data are given in Tables 3 and 4. Dashed lines show limits for r-I and r-II stars.

termine its orbit will be necessary to better constrain its mass loss. Still, for now we can at least conclude that it is plausible that Tuc III was once a more luminous galaxy than Ret II ($M_* = 2.6 \times 10^3$ $M_\odot$; Bechtol et al. 2015). We also cannot rule out the possibility that Tuc III had a luminosity as large as the other dwarfs with r-I stars before it ventured too close to the Milky Way.

If abundance measurements for a larger sample of Tuc III stars show a uniform level of r-process enrichment across the galaxy, that would point toward IGM pollution as the source of its r-process material. An internal spread in r-process abundances would most likely indicate that r-process elements were produced in Tuc III. If Tuc III contains a range of r-I and r-II stars similar to UMi and Draco, that may suggest that it was a much larger dwarf galaxy at earlier times before it was tidally stripped by the Milky Way. On the other hand, if most other Tuc III stars are not r-process enhanced, then much of the material responsible for enriching DES J235532 was likely ejected from the galaxy.

The astrophysical source of the r-process elements has been narrowed down, but is not yet conclusively identified. The current most promising sites are NSMs and jet-SNe, events that are similarly rare and that are equally able to reproduce the heavy neutron-capture element abundance pattern seen in r-process enhanced stars (Wanajo et al. 2014; Winteler et al. 2012). Tsujimoto & Shigeyama (2014) and Tsujimoto et al. (2015) argue that NSMs can produce the Eu abundances seen in dwarf galaxies, with a plateau seen in dwarfs that hosted no more than one NSM event and increasing Eu with Fe in the dwarfs where multiple NSMs have happened. However, an increasing trend is seen in both UMi and Ret II, which according to the Tsujimoto et al. (2015) model should show a plateau in their [Eu/H] abundances. Furthermore, some of the dwarfs showing an increasing trend in Eu with metallicity also show evidence of enrichment by the s-process, and thus the increase in Eu with metallicity in those systems may not be entirely due to r-process enrichment. With only one star

in Tuc III we cannot yet say whether the Eu abundances in this galaxy increase with metallicity, sit on a plateau, or behave in a different manner entirely. However, given its metallicity the [Eu/H] ratio of DES J235532 is consistent with those of other r-process enhanced stars in dwarf galaxies and in the halo.

The r-process enhanced stars from the individual dwarf galaxies each create a sequence in the left panel of Figure 5 (Fornax appears to contain two sequences). For the dwarf galaxies containing r-I stars these sequences fall on top of the area populated by the halo r-I stars, whereas the r-II stars in Ret II are seen at higher [Eu/H] ratios. This results in the [Eu/Fe] distribution seen in the right panel where the top peak is dominated by the Ret II stars. A more gradual transition is seen for the r-process enhanced stars in the halo. From the abundance cuts used to select r-I ($0.3 <$ [Eu/Fe] < 1, [Eu/Ba] > 0.4) and r-II ([Eu/Fe] > 1, [Eu/Ba] > 0.4) stars one would expect, with a large enough sample, to see a gradual transition between r-I and r-II stars at different metallicities, as is the case for the halo stars. For the r-stars in the dwarf galaxies the location of the [Eu/H] sequence may be a result of the level of dilution of the r-process ejecta. For example in the low luminosity dwarf Ret II only a small amount of gas was available to dilute the r-process ejecta, whereas the higher luminosity system UMi had a larger gas reservoir within which the r-process ejecta were mixed, creating similar sequences in [Eu/H], but with an offset. Thus in principle with a large sample of r-process enhanced dwarf galaxies of varying luminosity the gap between the Ret II stars and the r-process enhanced stars from other dwarf galaxies would be filled in.

The current sample of r-I and r-II stars in dwarf galaxies to our knowledge comprises 20 r-I stars in five different systems and 12 r-II stars in four different systems, with the majority of the r-II stars located in Ret II. This ratio of r-I stars to r-II stars is similar to what is found in the halo, where at present ~ 45 r-I and ~ 25 r-II stars have been identified. The r-I stars discovered in dwarf

galaxies so far seem to cover the more metal-rich end of the metallicity distribution of halo r-I stars. Similarly, the r-II stars identified in dwarf galaxies that contain r-I stars as well have metallicities of [Fe/H] ~ -2. One r-II star of similar metallicity ([Fe/H] $= -1.7$) has been detected in the MW bulge (Johnson et al. 2013), but no r-II stars at such high metallicities have yet been detected in the MW halo, where the known r-II stars are all at [Fe/H] ~ -3 (Barklem et al. 2005).

6. CONCLUSIONS

In this paper we have presented a full abundance analysis of the star DES J235532.66$-$593114.9 in the ultra-faint dwarf galaxy Tucana III. We find that DES J235532 is enhanced in r-process elements and classify it as an r-I star. This is the first r-I star to be identified in a dwarf galaxy of such low luminosity. After compiling a complete literature sample of dwarf galaxy r-I stars, we show that the heavy neutron-capture element abundance pattern of this star and r-I stars in other dwarf galaxies matches that of the classical r-II star CS 22892$-$052. The same match has been detected for r-I stars in the halo; it is therefore possible that the r-I stars currently located in the Milky Way halo were born in dwarf galaxies covering a range in luminosity such as Tuc III and Ursa Minor.

When comparing the dwarf r-I stars to halo r-I stars, we find that the majority of the halo stars are more metal-poor and Ca-rich than the r-I stars identified in dwarf galaxies. However, the sample size of known r-process enhanced stars in both the halo and in dwarf galaxies is still limited and many of the halo studies have been focused on the more metal-poor ([Fe/H] < -3.0) stars. Hence larger samples may reveal lower metallicity r-process enhanced stars in dwarfs and higher metallicity r-process enhanced stars in the halo.

Because of the very low luminosity of Tuc III it is surprising that the system contains any r-process-enhanced stars. Among other faint dwarfs only Reticulum II hosts such stars, while the other dwarf galaxies with known r-I stars all have stellar masses that are orders of magnitude larger. Both internal and external production of the r-process material in Tuc III are possible, but with abundance information for only a single star we cannot distinguish between them. High-resolution spectroscopy of a small number of additional stars in Tuc III, covering both the tidal tails and the core, will reveal whether, like Ret II, Tuc III was the location of a neutron star merger at early times, or if it was polluted by an outside r-process event.

Finally, we examine the [Eu/H] abundances for the r-process enhanced stars in dwarf galaxies and in the halo. It has been suggested that enrichment from NSMs should result in a plateau in the [Eu/H] abundances for stars in dwarf galaxies. While small samples may result in the appearance of such plateaus in individual objects, the combined sample from many dwarfs is consistent with a steady increase in [Eu/H] with metallicity. Parallel sequences in [Eu/H] for various galaxies, most notably Ret II and UMi, may correspond to the different levels of dilution of the r-process ejecta in each dwarf.

The discovery of r-process enhanced stars in ultra-faint dwarf galaxies presents us with an environmental constraint on the event(s) responsible for creating the heaviest elements in our Universe. With larger samples the differences and similarities in mass and history of the dwarf galaxies along with the abundance patterns of the r-process enhanced stars themselves can help constrain the astrophysical site of the r-process.

REFERENCES

Aoki, W., Beers, T. C., Christlieb, N., et al., 2007, ApJ, 655, 492

Arcones, A., Janka, H. D., & Scheck, L. 2007, A&A, 467, 1227

Arcones, A., & Thielemann, F, K., 2013, Journal of Physics G Nuclear Physics, 40, 1

Asplund, M., Grevesse, N., Sauval, A. J., & Scott, P., 2009, ARA&A, 47, 481

Barklem, P. S., Christlieb, N., Beers, T. C., et al., 2005, A&A, 439, 129

Bauswein, A., Goriely, S., & Janka, H. T. 2013, ApJ, 773, 78

Bechtol, K., Drlica-Wagner, A., Balbinot, E., et al. 2015, ApJ, 807, 50

Beers, T. C., & Christlieb, N., 2005, ARA&A, 43, 531

Bernstein, R., Shectman, S. A., Gunnels, S. M., Mochnacki, S., & Athey, A. E. 2003, Proc. SPIE, 4841, 1694

Bressan, A., Marigo, P., Girardi, L., et al. 2012, MNRAS, 427, 127

Cameron, A. G. W., 2003, ApJ, 587, 327

Carney, B. W., Latham, D. W., Stefanik, R. P., et al., 2003, AJ, 125, 293

Castelli, F. & Kurucz, R. L., 2003, IAU Symposium, 210

Chubak, C., Marcy, G., Fischer, D. A., et al. 2012, arXiv:1207.6212

Cohen, J. G. & Huang, W., 2009, ApJ, 701, 1053

Cohen, J. G. & Huang, W., 2010, ApJ, 719, 931

The Dark Energy Survey Collaboration et al. 2016, MNRAS, 460, 1270

Dotter, A., Chaboyer, B., Jevremović, D., et al. 2008, ApJS, 178, 89

Drlica-Wagner, A., Bechtol, K., Rykoff, E. S., et al. 2015, ApJ, 813, 109

Flaugher, B., Diehl, H. T., Honscheid, K., et al. 2015, AJ, 150, 150

François, P., Monaco, L., Bonifacio, P., et al. 2016, A&A, 588, A7

Frebel, A., Casey, A. R., Jacobsen, H. R., & Yo, Q., 2013, ApJ, 769, 57

Freiburghaus, C., Rosswog, S., & Thielemann, F. K. 1999, ApJL, 525, L121

Fuhr, J. R. & Wiese, W. L., 2009, Atomic Transition Probabilities, published in the CRC Handbook of Chemistry and Physics, 90th Edition, ed. Lide, D. R., CRC Press, Inc., Boca Raton, FL, 10-93

Fujimoto, S. I., Nishimura, N., & Hashimoto, M. A. 2008, ApJ, 680, 1350

Fulbright, J. P., Rich, R. M., & Castro, S. 2004, ApJ, 612, 447

Geisler, D., Smith, V. V., Wallerstein, G., Gonzales, G., & Charbonnel, C., 2005, AJ, 129, 1428

Goriely, S., Bauswein, A., & Janka, H. T. 2011, ApJL, 738, L32

Gratton, R., Sneden, C., & Carretta, E. 2004, ARA&A, 42, 385

Griffen, B. F., Dooley, G. A., Ji, A. P., et al. 2016, submitted to MNRAS (arXiv:1611.00759)

Hansen T., Andersen, J., Nordström, B., Beers, T. C., Buchhave, L. A. & Yoon, J., 2015, A&A, 583, A49

Hansen T., Andersen, J., Nordström, B., Buchhave, L. A., & Beers, T. C., 2011, ApJ, 743, L1

Hill, V., Plez, B., Cayrel, R., et al., 2002, A&A, 387, 560

Jablonka, P., North, P., Mashonkina., et al., 2015, A&A, 583, A67

Ji, A. P., Frebel, A., Chiti, A. & Simon, J. D., 2016a, Nature, 531, 610

Ji, A. P., Frebel, A., Simon, J. D., & Chiti, A. 2016b, ApJ, 830, 93

Johnson, C. I., McWilliam, A., & Rich, R. M., 2013, ApJ, 775, L27

Kelson, D. D. 2003, PASP, 115, 688

Kirby, E. N. & Cohen, J. G., 2012, AJ, 144, 168

Komiya, Y., & Shigemeyama, T., 2016, ApJ, 830, 76

Koposov, S. E., Belokurov, V., Torrealba, G., & Evans, N. W. 2015, ApJ, 805, 130

Korobkin, O., Rosswog, S., Arcones, A., & Winteler, C. 2012, MNRAS, 426, 1940

Lattimer, J. M. & Schramm, D. N. 1974, ApJL, 192, L145

Lemasle, B., de Boer, T. J. L., Hill, V., et al., 2014, A&A, 572, A88

Letarte, B., Hill, V., Tolstoy, E., et al., 2010, A&A, 523, A17

Masseron, T., Plez, B., Van Eck, S., et al., 2014, A&A, 571, A47

McWilliam, A., Preston, G. W., Sneden, C., & Searle, L., 1995, AJ, 109, 2757

McWilliam, A., Wallerstein, G., & Mottini, M., 2013, ApJ, 778, 149

Metzger, B. D., Martínez-Pinedo, G., Darbha, S., et al. 2010, MNRAS, 406, 2650

Meyer, B. S. 1989, ApJ, 343, 254

Peñarrubia, J., Navarro, J. F., & McConnachie, A. W. 2008, ApJ, 673, 226-240

Placco, V. M., Frebel, A., Beers, T. C., & Stancliffe, R. J., 2014, ApJ, 797, 21

Qian, Y.-Z. & Wasserburg, G. 2001, ApJ, 552, L55

Ramírez, I., Allende Prieto, C., & Lambert, D. L., 2013, ApJ, 764, 78

Roederer I. U., Cowan, J. J., Preston, G. W., Thompson, et al., 2014b, MNRAS, 445, 2970

Roederer, I. U., Marino, A. F., & Sneden, C. 2011, ApJ, 742, 37

Roederer, I. U., Mateo, M., Bailey, J. I., III, et al. 2016, AJ, 151, 82

Roederer I. U., Preston, G. W., Thompson, I. B., et al., 2014, AJ, 147, 136

Rosswog, S., Korobkin, O., Arcones, A., Thielemann, F. K., & Piran, T. 2014, MNRAS, 439, 744

Ryabchikova, T., Piskunov, N., Kurucz., et al., 2015, Phys. Scr, 90, 5

Sadakane, K., Arimoto, N., Ikuta, C., Aoki, W., Jablonka, P. & Tajitsu, A., 2004, PASJ, 56, 1041

Shetrone, M. D., Côté, P. & Sargent, W. L. W., 2001, ApJ, 548, 592

Shetrone, M. D., Venn, K. A. Tolstoy, E., Primas, F., Hill, V., & Kaufer, A., 2003, AJ, 125, 684

Simmerer, J., Sneden, C., Cowan, J. J., et al., 2004, ApJ, 617, 1091

Simon, J. D., Jacobson, H. R., Frebel, A., et al., 2015, ApJ, 802, 93

Simon, J. D., Li, T. S., Drlica-Wagner, A., et al. 2016, ApJ in press (arXiv:1610.05301)

Siqueira Mello, C., Hill, V., Barbuy, B., et al., 2014, A&A, 565, A93

Siqueira Mello, C., Spite, M., Barbuy, B., et al., 2013, A&A, 550, A122

Skúladóttir, Á., Tolstoy, E., Salvadori, S., et al., 2015, A&A, 574, A129

Sneden, C., 1973, ApJ, 184, 839

Sneden, C., Cowan, J. J. & Gallino, R., 2008, ARA&A, 46, 241

Sneden, C., Cowan, J. J., Lawler, J. E., et al., 2003, ApJ, 591, 936

Sobeck, J. S., Kraft, R. P., Sneden, C., et al., 2011, AJ, 141, 175

Tafelmeyer, M., Jablonka, P., Hill, V., et al., 2010, A&A, 524, A58

Tsujimoto, T., Ishigaki, M. N., Shigeyama, T., & Aoki, W. 2015, PASJ, 67, L3

Tsujimoto, T., & Shigeyama, T., 2014, A&A, 565, L5

Venn, K. A., Shetrone, M. D., Irwin, M. J., et al., 2012, ApJ, 751, 102

Wanajo, S., Sekiguchi, Y., Nishimura, N., 2014, ApJ, 789, L39

Winteler, C., Käppeli, R., Perego, A., et al., 2012 ApJ, 750, L22

Yong, D., Meléndez, J., Grundahl, F., et al. 2013, MNRAS, 434, 3542